UCRL-JC-123573
PREPRINT
CONF-951182--13

Critical Tests of Line Broadening Theories by Precision Measurements

S. H. Glenzer

This paper was prepared for submittal to
37th Annual Meeting of the APS Division of Plasma Physics
Louisville, KY
November 6-10, 1995

February 22, 1996

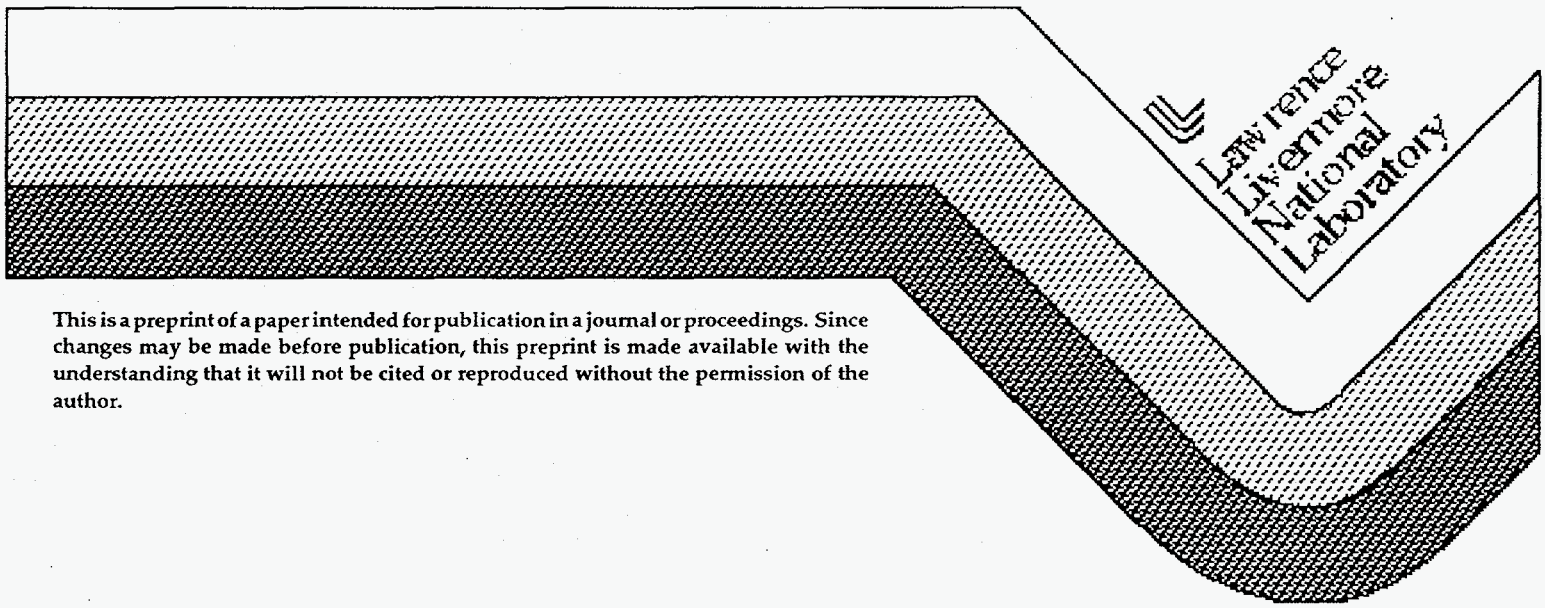

Critical Tests of Line Broadening Theories by Precision Measurements

Siegfried H. Glenzer

Institut für Experimentalphysik V, Ruhr-Universität, 44780 Bochum, Germany
present address: Lawrence Livermore National Laboratory L-399, University of California, P.O. Box 808, Livermore, CA 94551, USA

Abstract. We describe recent measurements of spectral line profiles of a z-pinch experiment employing precision plasma diagnostic techniques. In particular, the electron-collisional-broadened 2s - 2p transitions in B III have been investigated because their line profiles provide an excellent test for electron-impact line shape theories and electron collision strength calculations. Although we find good agreement with semiclassical calculations, a factor of two discrepancy with the most elaborate quantum-mechanical five-state close coupling calculations is observed. We discuss the experimental error estimates of the various measured quantities and show that the observed discrepancy can not be explained by experimental shortcomings. We further discuss measurements of non-isolated spectral lines of some $\Delta n = 1$ transitions in C IV - O VI. For these transitions ion broadening dominates. Excellent agreement for the whole line profile with line broadening calculations is obtained for all cases only when including ion dynamic effects. The latter are calculated using the frequency-fluctuation model and account for about 10 - 25 % of the line width of the considered ions.

INTRODUCTION

The spectral line profiles of ionized emitters in plasmas play an important role in the calculation of opacity (1,2), for short-wavelength laser studies (3), and for the diagnostics of inertial confinement fusion plasmas (4-6). Sophisticated theoretical methods and modeling have been advanced and applied in recent years (7-9) to calculate spectral line profiles in the limits where broadening by electron collisions or by ion microfields dominates.

Electron collisional broadening dominates the line broadening of isolated spectral lines of nonhydrogenic emitters. In most cases the impact approximation is valid over the frequency range of the spectral line profiles. The criterion (10) for the validity of the impact approximation is that the duration of the collision of the perturber with the emitter τ is much smaller than the inverse of the half-width at half maximum ϖ or the inverse of the angular frequency separation $\mid \Delta\omega \mid$ from the line center

$$\tau = \frac{\rho}{v} \ll min\left(\frac{1}{\mid \Delta\omega \mid}, \frac{1}{\varpi}\right); \qquad (1)$$

ρ is the impact parameter and v is the velocity of the electron. The general solution is a Lorentzian with a full-width at half maximum w given by the rates of effective (electron) collisions (11). Baranger used the optical theorem to derive the following expression

$$w = \left\{ n_e v \left(\sum_{u' \neq u} \sigma_{uu'} + \sum_{l' \neq l} \sigma_{ll'} + \int \mid \Phi_u - \Phi_l \mid^2 d\Omega \right) \right\}_{av} . \qquad (2)$$

This equation shows explicitly the contributions to the linewidth from inelastic electron collisions by summing over the cross sections of electron collisions between levels involving the upper ($\sigma_{uu'}$) and lower ($\sigma_{ll'}$) states of the transition of interest, and from a term taking into account elastic scattering by subtracting the scattering amplitudes Φ of the initial and final level and integrating over the scattering angle $d\Omega$. In most practical cases the average is over a Maxwell-Boltzmann velocity distribution function.

Equation (2) shows the correlation between spectral line shape calculations and atomic collision theory. Some recent progress on line broadening calculations came from this field where collision strength or cross sections are now routinely calculated with a variety of advanced methods. In particular, within the Opacity Project close-coupling calculations have been performed to calculate collision strengths and line widths for a large number of transitions. These calculations are expected to be the most accurate theoretical data because semiempirical (12) or semiclassical (10,13,14) approximations use *ad hoc* estimations for the effective Gaunt factor to account for elastic electron collisions. Further, similar crude assumptions are also necessary within a semiclassical theory to account for strong collisions (8,10,13). On the other hand, there are a lack of reliable experiments testing close-coupling calculations. It is obvious from Equation (2) that measurements of spectral line widths from isolated nonhydrogenic ions in well-diagnosed plasmas can provide critical tests of calculations of effective (elastic and inelastic) cross sections. Some experiments (15,16) have been performed in discharge tubes which were diagnosed with interferometry. But, as pointed out by Seaton (7) the experimental data were not accurate or convincing enough to provide a critical test for close-coupling calculations.

For that reason we have performed new experiments (17,18) with the well-diagnosed gas-liner pinch where electron densities and temperatures are determined independently with Thomson scattering. Furthermore, no assumptions about homogeneity of the plasma or radiative transport effects are necessary, because we have been able to directly measure electron and emitter density distributions in the plasma. Our measurements include the $2s - 2p$ resonance transitions in B III since their line profiles are excellent test objects of close-coupling calculations (18). It is the simplest system to calculate since there is only one electron outside the first shell. Moreover, for these transitions between lowly excited states the inclusion of only a small set of perturbing levels should lead to high accuracy.

For especially broad spectral lines the duration of a given perturbation assumes the same order as the decay time of the autocorrelation function of the light amplitude, and no general solution of the spectral line profile similar to Equation (2) can

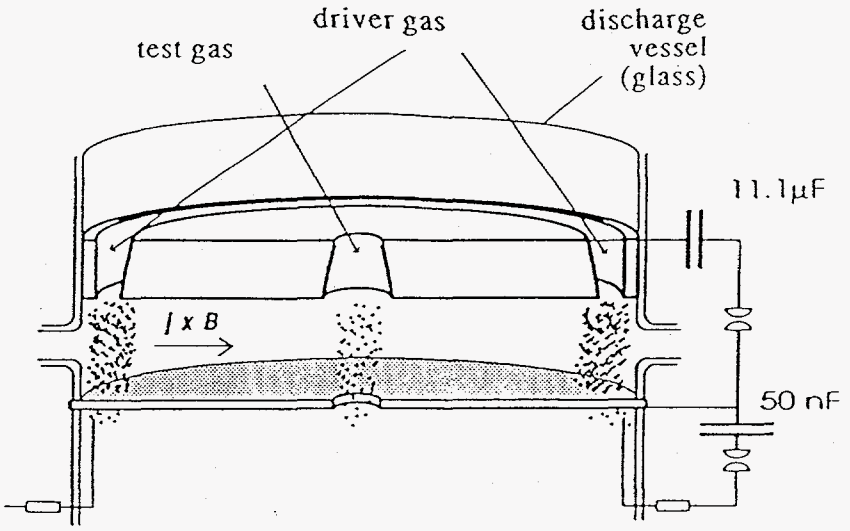

Figure 1. Schematic of a gas-liner pinch.

be given. In particular, broadening by ion microfields becomes more important and in the limit where Equation (1) is reversed, the quasi-static (ion) approximation can be applied (10,19). More often, however, Equation (1) is only reversed for the wings of the line profile and for the central part of the profile ion dynamic corrections have to be taken into account. For example, this is the case for some non-isolated $\Delta n = 1$ transitions of the lithium-like ions C IV, N V, and O VI for transitions of more highly excited states which have close-lying perturbing levels (20,21). We tested complete spectral line profile calculations which were performed for the independently measured plasma parameters of our experiment.

EXPERIMENT AND DIAGNOSTIC TECHNIQUES

GAS-LINER PINCH. A gas-liner pinch resembles a large aspect ratio $z-$pinch characterized by two independent fast gas inlet systems (22). Figure 1 shows the experimental setup. For the present investigations we used hydrogen or helium as driver gas. It is injected through an annular nozzle into the vacuum chamber by a fast electromagnetic valve. The diameter of the vacuum chamber is 18 cm and the electrode separation is 5 cm. The gas forms a hollow gas cylinder near the wall before we preionize it by discharging a 50 nF-capacitor (charged to 20 kV) between 50 annuarly mounted needles and the lower cathode. Finally, the discharge of the main capacitor (capacitance 11.1 μF, voltage 25-35 kV) compresses the gas on axis to a plasma column of 1-2 cm diameter and 5 cm length. Typical electron densities and temperatures reached on the axis are between $0.5 < n_e < 4 \times 10^{18}\mathrm{cm}^{-3}$ and $7.5 < k_B T_e < 50$ eV which is sufficiently hot and dense to produce multiply ionized atoms with Stark broadening as the dominant broadening mechanism of their emission lines. The compression time and the life time of the plasma depend on the discharge conditions and for the present studies they are about 2.5 μs and 0.5 μs, respectively.

The atomic species of interest for spectroscopic measurements are introduced as (test) gas into the discharge tube by a second independently operating fast electromagnetic valve. The gas is injected through a nozzle in the center of the upper electrode and is dissociated and ionized by the imploding driver gas and by ohmic heating. For the present studies we used BF_3, CH_4, N_2, CO_2, a mixture of 10 % SF_6 in hydrogen or Ne as test gas in order to produce the lithium-like ions B III, C IV, N V, O VI, F VII, and Ne VIII. Their radial emission is observed with several spectrometers for the visible and vacuum ultraviolet spectral range. Gated microchannel plates and optical multichannel analyzers or charge-coupled devices were used to perform all measurements with a time resolution of 20 - 30 ns.

THOMSON SCATTERING. An independent and accurate measurement of all relevant plasma parameters is a prerequisite for a critical test of line shape theories. For this purpose we focussed a pulse of a Q-switch driven Ruby laser (2 J, 30 ns) into the center of the plasma column and observed the scattered light at an angle of $\theta = 90°$. This arrangement gives typical values for the scattering parameter $\alpha = 1/(k\lambda_D) > 1$. In this regime light is predominantly scattered into a narrow ion feature which could be detected spectrally resolved with a 1-m spectrometer and a gated optical multichannel analyzer. Scattering occurs on electrons which are bunched in the Debye spheres of the ions, and from the width of the scattering spectrum the temperature of the ions is obtained. Furthermore, on the wings of the ion feature, heavily-damped ion acoustic waves determine the shape of the scattering spectrum. Since the phase velocity and the damping of ion acoustic waves depend on the ion and on the electron temperature, an accurate measurement of the shape of the scattering spectrum also yields the electron temperature.

By calibrating the detection system absolutely by Rayleigh scattering on propane the electron density is deduced from the intensity of the scattering spectrum. For the present investigations multiply ionized test gas atoms are added to the plasma column which is predominantly formed by the driver gas. Hence, we fit the theoretical form factor of Evans (23) to the measured scattering spectra. This form factor calculates the scattering spectra for a plasma composed of different ionic species. We gave a complete discussion applying this form factor to deduce the plasma parameters in Ref. (24).

In general, we obtain that the temperatures of all species are equal within the stated error of about 15 %. This finding is expected from estimates of the electron-ion collision time (25) resulting in typical values of about 3 ns. This is much smaller than typical time scales on which plasma parameters change after stagnation on the axis, i.e. after the maximum compression of the plasma. Figure 2 shows an example of a measured Thomson scattering spectrum along with the fitted form factor. This measurement was performed with hydrogen as driver gas and borontrifluoride as test gas. An impurity peak from test gas ions, which was easily observed in Refs. (26,27) when using larger amounts of test gas and more highly ionized species, can not be identified in Fig. 2. This is because only very small amounts of borontrifluoride have been used for the investigation of the line profiles of the $2s-2p$ resonance transitions

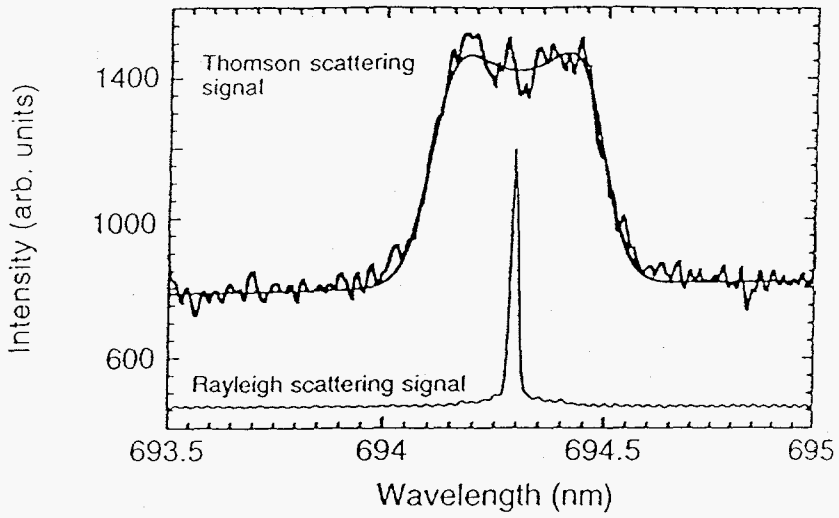

Figure 2. Example of a Thomson scattering spectrum detected 50 ns after maximum pinch compression along with the fit.

in order to avoid self-absorption. An upper limit for the test gas ion concentration n_t can be determined: $n_t < 0.3$ % of the electron density.

In Fig. 2 we also show a Rayleigh scattering spectrum obtained from light scattering on propane. We performed these type of calibration (about 20 measurements) after each shot day and monitor the small changes of the sensitivity of the detection system over several months resulting in a high reliability of the calibration. These measurements are carried out in the pulsed mode of the detector, or in other words in the same configuration as the Thomson scattering or the line broadening setup. Therefore, the Rayleigh scattering signal directly provides a measurement of the instrument function of the spectrometers for the visible spectral range: a Voigt function with 0.0071 nm Lorentzian FWHM and 0.0049 nm Gaussian FWHM. As usual we perform Rayleigh scattering for a variety of different propane gas densities, and besides checking the linerarity of the scattering and of the detection system, the instrument function is obtained for the full dynamic range of the detector. We should mention that the instrument function obtained in this way is in excellent agreement with the measurement performed in the cw mode of the detector employing cold spectral lamps and Fe and Al hollow cathode lamps.

PLASMA HOMOGENEITY AND RADIATIVE TRANSPORT. Very favorable plasma conditions for line broadening studies are achieved when the injection of the gases into the discharge chamber is properly timed and only when very small amounts of test gas (about 1 % of the density of the driver gas) are used. The test gas ions become confined in the center of the plasma column where the plasma is homogeneous in radial and axial direction.

Experimentally we have verified the plasma homogeneity with various methods (17,27,28). Electron densities from Thomson scattering as a function of the radius

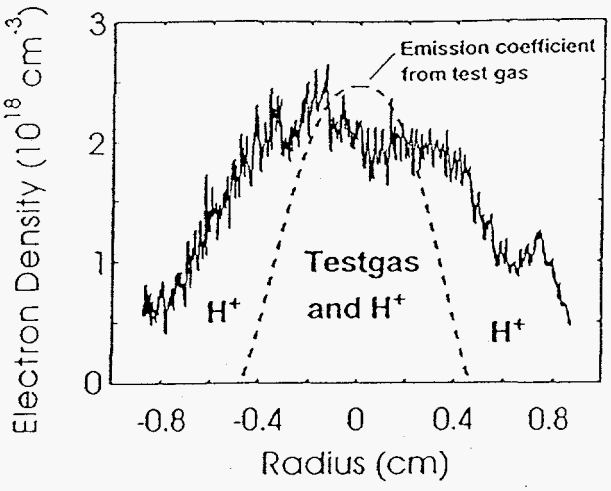

Figure 3. Electron density as a function of the radius of the discharge. The dashed line represents the emission coefficient for line radiation emitted from test gas ions.

show that the emission from test gas ions originates from a homogeneous center of the plasma column with about 1 cm diameter. Figure 3 shows a result obtained shortly after maximum pinch compression. Also shown is the emission coefficient of line radiation from test gas ions obtained after Abel inversion.

It is further of interest to verify the homogeneity of the plasma column in axial direction because magnetohydrodynamic instabilities could arise. We measured the homogeneity along the axis of the discharge in two different experiments (25). In Fig. 4 we show the Stark-broadened $n = 5$ to $n = 4$ transitions of F VII at $\lambda = 82.5$ nm. These linewidths are very sensitive to changes of the electron density but insensitive to temperature variations. Temporally and axially resolved spectra have been detected from single discharges at various times in the discharge with a MCP-CCD system. Figure 4 shows an example of a measurement at maximum pinch compression. About 1 cm of the 5 cm long plasma column is shown with a resolution of 0.17 mm. In order to derive the electron density from the line profiles we determined the full-widths at half maximum of the transitions as a function of the height of the plasma with a resolution of 0.5 mm. We converted the linewidth obtained in this way into electron densities using spectral line broadening calculations (see Ref. (9))and which are tested below. The rms value is 14 % of the mean value of the electron density. The homogeneity of the discharge is evident.

For transitions with highly populated lower levels self-absorption is a serious problem which leads to line profile distortions. In particular, this is true for resonance transitions. Since at our experimental conditions the plasma is homogeneous and a cold boundary layer of the investigated ions is effectively absent, radiative transport effects of the emission lines are easily controlled by varying the amount of test gas. In fact, optically thin plasma conditions for all line broadening measurements were achieved. This is expected from the measurement of the emitter density with Thomson scattering which is, e.g., about 0.3 % of the electron density for the

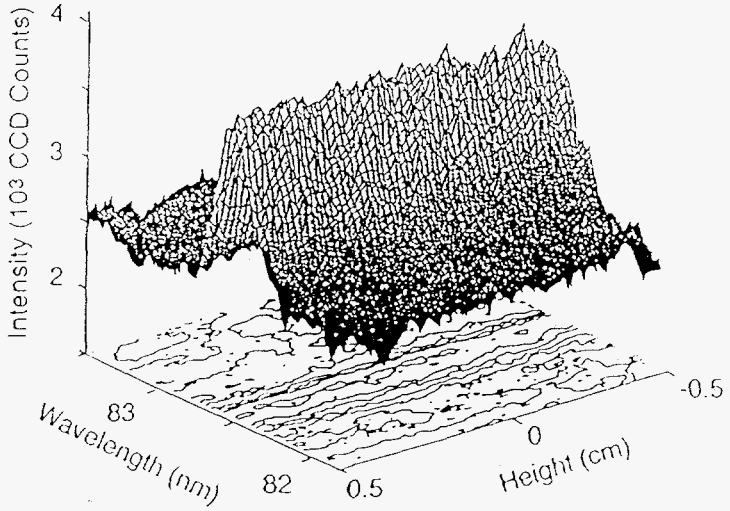

Figure 4. Example of a MCP-CCD measurement of the $n = 5 - n = 4$ transitions in F VII as a function of the height of the pinch.

boron measurements. We further verified that radiative transport is negligible by measuring relative line intensities within multiplets for different plasma conditions and test gas ion concentrations. Since the high particle densities of a gas-liner pinch plasma result in sufficiently high collision rates, level population densities within a multiplet are given by the Boltzmann statistics. Hence, we compare measured line intensities with the predictions of the LS-coupling approximation.

We find for the investigated Li-like ions B III - Ne VIII that the measured line intensity ratios of the $2s - 2p$ or $3s - 3p$ transitions are in good agreement with the predictions of the LS-coupling approximation (see also Figure 5). The predicted ratios are within the measured uncertainties of about 3 %. Also, increasing the test gas concentration by a factor of 2 did not affect this result.

EXPERIMENTAL RESULTS AND DISCUSSION

Figure 5 shows an example of a spectrum of the $2s - 2p$ resonance transitions of B III detected 50 ns after maximum pinch compression. Also shown is a fitted Voigt function which takes into account the instrument function and Doppler broadening in the following way: the measured instrument profile (see Fig. 2) is convoluted with a Doppler profile which was calculated for each plasma condition according to the measured temperature. The resulting profile is convoluted with a Lorentzian with a variable width giving the Stark broadening. Both multiplet lines are fitted independently giving for each spectrum the same width for both components within 5 %. For each spectrum the relative intensities of both components is $2 : 1 \pm 4$ %, in excellent agreement with the LS-coupling approximation predicting 2.00 : 1.00. Both facts show that there are no unwanted detector distortions for the high intensity line and that the measurement is not affected by self-absorption. For the condition in Fig. 5 we obtain for the Stark broadening $w_m = 0.022$ nm $\pm$ 11.5 %.

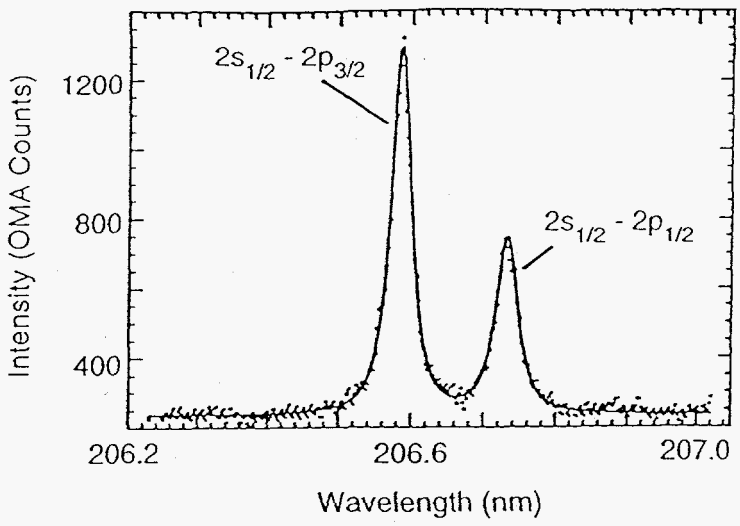

Figure 5. Experimental spectrum of the $2s - 2p$ multiplet of B III measured 50 ns after maximum pinch compression; ■, experimental data; —, Voigt function best fit. Electron densities and temperatures are obtained from Thomson scattering.

For the narrow resonance transitions of B III sufficiently high resolution of the detection system is obtained by going to the 6th spectral order and using an interference filter to suppress the radiation from all other orders. The filter has equal transmission over the wavelength range of interest as proven with hydrogen continuum measurements. For our experimental conditions the instrument and the Doppler profile together account for 33 % of the measured linewidth. Hence, uncertainties in the measurement of these quantities increases the error of the Stark broadening measurement. The instrument profile is more critical because it contributes directly to the Lorentzian contribution of the measured spectra. Fortunately, the instrument profile is measured very accurately and on a frequent basis, and therefore, only the experimental error in the determination of the temperature of the plasma results in an uncertainty of the Gaussian contribution of the measured line profiles. Since temperatures are also measured with high accuracy with Thomson scattering and since the Gaussian contribution is less important for the width of the resulting Voigt functions, the additional error from the Gaussian contribution is only 2 %. This error is added to the rms value of the fitted Stark profiles of 10 spectra measured at the same plasma condition. It results in a total error for the experimental Stark width of 13.5 %.

Stark width are usually calculated for a series of temperatures and for one value of the electron density. This is because it is a fundamental concept of the impact theory that the contribution to the linewidth owing to electronic or ionic collisions is proportional to their number density (10,11) (see Equation (2)). Indeed, a linear scaling of linewidths of nonhydrogenic ions has been proven in a number of experiments (10,15). In practical situations, deviations from a linear scaling may be possible due to Debye shielding effects (10,29) which are, however, unimportant for this study (30). For that reason we can scale the experimental or theoretical Stark

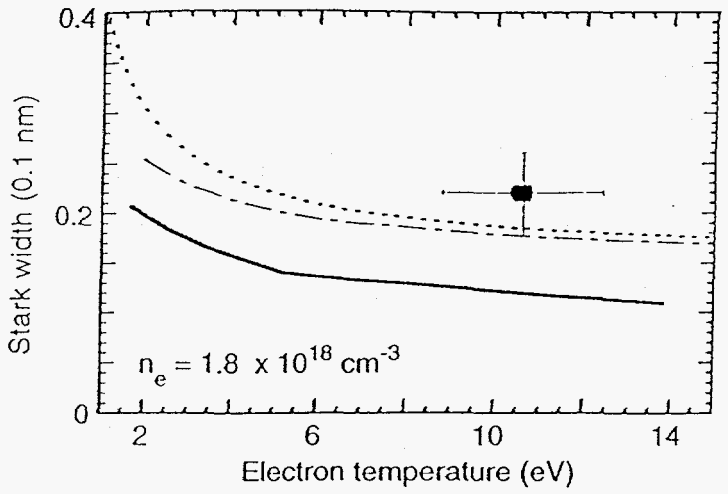

Figure 6. Comparison of the experimental Stark width (FWHM) of the $2s - 2p$ transitions in B III with the results of the theoretical approximations after Griem (10): ····, by Hey and Breger (13): - - - - -, and from Seaton (7): — . The vertical error bar takes into account the errors of the measured line profiles, of the convoluted Doppler profile, and of the electron density determination.

width linearly to one value of the electron density. Hence, for a comparison with theory the experimental errors of the measured electron density have to be taken into account. Plasma parameters are measured independently with Thomson scattering, and for the B III study the rms values result in a relative error in the density and in the temperature of 13 % and 16 %, respectively. Since the measurements of the linewidths and of the electron densities are independent and statistical, combining both errors for a comparison with theory amount to 20 % of the Stark width.

In Figure 6 we compare our experimental result to various theoretical data which are plotted as a function of the electron temperature. The measured electron density is $n_e = 1.81 \times 10^{18}\text{cm}^{-3}$. The results of two semiclassical approximations according to Griem (10) and to Hey and Breger (13), and close-coupling calculations from Seaton (7) are shown. These theoretical approximations calculate only electron-impact widths. The semiclassical approximation after Griem (10) calculates inelastic cross sections with good accuracy for impact parameters larger than the extent of the wavefunction of the perturber, i.e. in a regime where the semiclassical approximation is valid. Collisions with smaller impact parameters are estimated with a Lorentz-Weisskopf term and give the so-called strong collision term which is 12 % of the total calculated width. A maximum impact parameter of the order of the Debye length, and elastic contributions are included according to an extrapolation procedure below threshold. Hey and Breger (13) chose different procedures from those of Griem (10) to calculate the minimum and maximum impact parameters of the electron collision process. Although their strong collision term is appreciably larger, even for the relatively low charge state of the studied ion, their resulting widths differ only slightly from that of Griem. Both semiclassical calculations agree with the

experiments within the 20 % error bar.

On the other hand, the close-coupling calculations give results which are smaller than the experiment by a factor of about two. This discrepancy can not be explained by other broadening mechanisms besides electron-impact broadening because those broadening mechanisms can account for only a few percent of the measured width. Ion broadening is almost negligible for the resonance lines of B III. Griem gives a relatively large rough estimate of the ion quadrupole broadening (Eq. 218b, Ref. (10)). This term is about 10 % of the calculated electron-impact width but is not included in the comparison of Figure 6 because it is too roughly known. More recent detailed calculations of the ion quadrupole broadening of the $3s - 3p$ transitions of the Li-like ions C IV – Ne VIII from Ref. (31) show that this additional broadening contribution can be appreciably smaller than Griem's estimate and is smaller than 5 % of the electron-impact width. Dipole-allowed proton collisions are completely negligible for the B III experiment (8,10), as is Zeeman broadening.

Moreover, we consistently find that semiclassical Stark width calculations are in better agreement with our experimental results than close-coupling calculations. We performed a detailed study for the $3s - 3p$ transitions in the Li-like ions C IV – Ne VIII (17,27). Our experimental results scaled to one value for the electron density and temperature, i.e. $n_e = 1.8 \times 10^{18}$ cm^{-3} and $k_B T_e = 12.5$ eV, are shown in Fig. 7. The error bars include the error from the width measurement, the electron density and temperature. Also, an error estimate for the scaling of the data is taken into account (17). For Ne VIII two experiments have been performed because for this transition proton collision broadening plays a role. One data point is obtained from experiments with hydrogen and one with helium as driver gas. The difference between both values gives an estimate for the magnitude of the proton collision contribution to the linewidth. We find for all transitions that the five-state close-coupling calculations give results which are too small to explain the measured widths. This finding might be partially explained by the fact that only five states are included in the calculations ($n = 2$ and $n = 3$ levels). While the $n = 4$ states do not contribute to the Stark broadening of the $2s - 2p$ resonance transitions in B III, they are expected to play a role for the $3s - 3p$ transitions in Li-like ions. Indeed, the nine-state close-coupling calculations from Burke (33) give an improved value for the Stark width of C IV which is marginally inside of the error bar of the experiment. However, the overall comparison of quantum-mechanical calculations with our experiments is not satisfactory, while comparisons with semiclassical calculations show generally good agreement. Until recently there have been problems explaining the experimental Stark width of the higher ionized emitters. A simplified Z^{-2} scaling as predicted by some theoretical approximations could not be verified by our experiments (see also Ref. (28)). On the other hand, the new semiclassical method of Alexiou (32,34) gives good agreement with the experiment for all investigated transitions. As opposed to other theoretical approximations Alexiou calculates the collision operator exactly for impact parameters in the region where unitarity is violated but the semiclassical approximation is still valid. This is done by a fully numerical solution of the Schrödinger equation. In fact, this method gives excellent agreement with our experimental data.

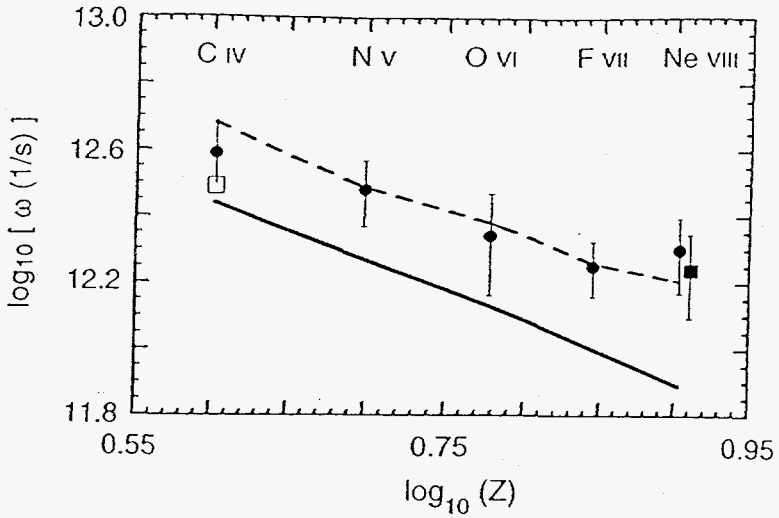

Figure 7. Experimental and theoretical Stark width in frequency units of the $3s\ ^2S - 3p\ ^2P^o$ transition in C IV – Ne VIII as function of Z: —, calculations by Seaton (7) (the values for N V and F VII are interpolated); □, calculated by Burke (33) ; - - -, calculations by Alexiou (8,31,32); experimental values (17,27): •, measured with hydrogen as driver gas; ■, measured with helium as driver gas.

Inaccuracies when deriving Stark widths from close-coupling calculations may arise because of large cancellations of direct and mixed terms (16) when calculating (1 - S_a S_b). Further approximations are the use of Hartree-Fock target states and the so-called top-up procedure where contributions from orbital quantum numbers $L > 16$ are only roughly estimated. An indication that these features indeed lead to problems in the calculation is the fact that two close-coupling calculations of the Stark broadening of the $2s - 2p$ resonance transitions in Be II performed by two different authors differ by a factor of 1.4 for low temperatures. On the other hand, we have the success of the semiclassical calculations. For example, from a large number of experiments with a broad range of experimental errors Konjević and Wiese (15), and Griem (10) find that the semiclassical approximation of Griem describes the Stark broadening of isolated spectral lines of two and three times ionized nonhydrogenic emitters within 50 %. From 28 independent experiments (17,28,30) with the well-diagnosed gas-liner pinch we find an even better agreement with the semiclassical calculations after Griem (10)

$$\frac{w_m}{w_G} = 0.92 \pm 26\ \% \tag{3}$$

and after Hey and Breger (13)

$$\frac{w_m}{w_{HB}} = 1.15 \pm 29\ \%. \tag{4}$$

So far we were concerned with isolated spectral lines of nonhydrogenic ions. Re-

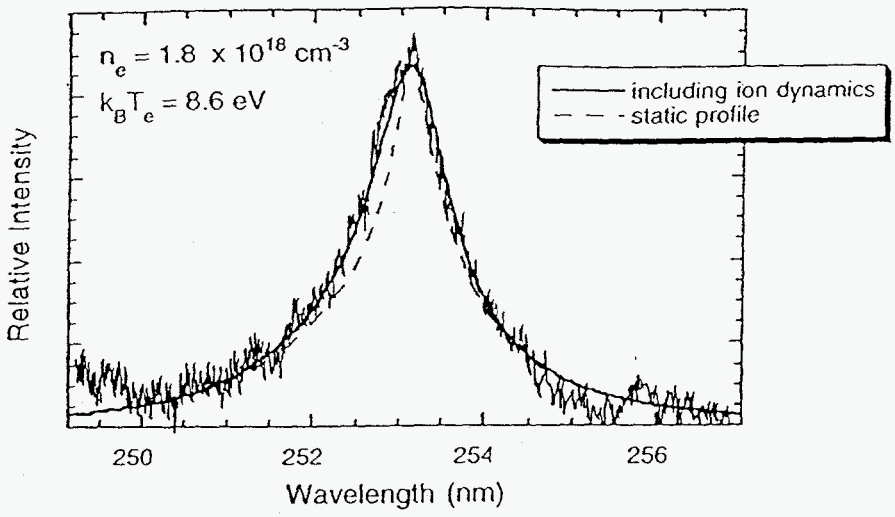

Figure 8. Experimental spectrum of the $n = 5$ to $n = 4$ transitions in C IV compared with independent calculations including static (- - -) and dynamic (—) ions. Electron densities and temperatures are obtained from Thomson scattering.

cently, we measured detailed line shapes of non-isolated spectral lines of lithium-like ions going to $\Delta n = 1$ transitions of more highly exited states with close-lying perturbing levels (21). In particular, we measured the $4f - 3d$ and $4d - 3p$ transitions of C IV and N V, and the $n = 5$ to $n = 4$ transitions in C IV, N V, and O VI. Due to the electric fields in the plasma the wave functions of the atomic states mix and become degenerate. Therefore, ion broadening dominates the line broadening. For these spectra forbidden transitions and overlapping of various $(n-1,\ell') - (n,\ell)$ transitions occur. Furthermore, ion-collisional effects at the center of the transitions, where the quasi-static ion approximation breaks down, have to be taken into consideration. Independent line profile calculations for the electron densities and temperatures measured with Thomson scattering have been performed taking into account these effects. A comparison with our experimental line profiles is shown in Figure 8 where the $n = 5$ to $n = 4$ transitions of C IV at 252.7 nm are plotted together with a calculated static and dynamic line profile. It is obvious that the latter, where ion dynamic effects are calculated using the field fluctuation model, is in much better agreement than the static profile. In this case the ion dynamic effect accounts for 25 % of the linewidth. From nine experiments performed with the gas-liner pinch we find that the field fluctuation model agrees excellent with the experimental line widths

$$\frac{w_m}{w_{ffm}} = 0.99 \pm 5\ \%. \tag{5}$$

In particular, in the central part of the transitions, agreement between the calculations and the experiments is obtained only when including ion dynamics, which accounts for 10 - 25 % of the linewidths. While ion dynamic effects have been found earlier to be important for hydrogen spectral lines this is the first decisive verification that ion dynamic effects can be also important for more highly ionized emitters.

CONCLUSIONS

For electron collisional broadened spectral lines we find that our experimental data of several studies clearly favor semiclassical calculations over five-state quantum-mechanical close-coupling calculations. In particular, the semiclassical calculations of Griem (10) and of Hey and Breger (13) agree well with the experiment for lowly ionized species. For more highly ionized emitters only the recent improvements of the semiclassical approximation (32,34) lead to satisfying agreement with our experimental data (17,34). Our experiments also include the best test case for close-coupling calculations: the $2s - 2p$ resonance transitions in the lithiumlike ion B III where a factor of two discrepancy between the close-coupling calculations and experiment is found (18). Since *a priori* the close-coupling calculations are considered to be most accurate it is imperative to understand this failure of close-coupling calculations before continuing to calculate more complicated systems.

For transitions where ion broadening dominates extensive studies show that the field fluctuation model developed in Refs. (4,9) agrees well with our experiments (20,21). In particular, we find for the first time that ion dynamic effects are important to describe the line profiles of more highly ionized emitters (21).

ACKNOWLEDGMENTS

I would like to thank H.-J. Kunze for many valuable discussions. I further thank C. A. Back, R. W. Lee, Th. Wrubel, and S. Büscher for helpful criticism. This research was supported by the Sonderforschungsbereich 191 of the DFG and DOE by LLNL under contract no. W-7405-Eng-48.

REFERENCES

1. Seaton M. J., J. Phys. B 20, 6363-6378 (1987).
2. Rogers F. J. and Iglesias C. A., Astrophys. J. Suppl. Series, 79, 507-568 (1992)
3. Koch J. A., MacGowan B. J, Da Silva L. B., Matthews D. L., Underwood J. H, Batson P. J., and Mrowka S., Phys. Rev. Lett. 68, 3291-3294 (1992).
4. Keane C. J., Lee R. W., Hammel B. A., Osterheld A. L., Suter L. J, Calisti A., Khelfaoui F., Stamm R., and Talin B., Rev. Sci. Instrum. 61, 2780-2783 (1990).
5. Hammel B. A., Keane C. J., Cable M. D., Kania D. R., Kilkenny J. D., Lee R. W., and Pasha R., Phys. Rev. Lett. 70, 1263-1266 (1993). Hammel B. A., Keane C. J., Dittrich T. R., Kania D. R., Kilkenny J. D., Lee R. W., and Levedahl W. K., J. Quant. Spectrosc. Radiat. Transfer 51, 113-124 (1994). N. Woolsey et al., *submitted to Phys. Rev. E*
6. Griem H. R., Phys. Fluids B 4, 2346-2361 (1992).
7. Seaton M. J., J. Phys. B 21, 3033-3053 (1988).
8. Alexiou S., Phys. Rev. A 49, 106-119 (1994).
9. Talin B., Calisti A., Godbert L., Stamm R., and Lee R. W., Phys. Rev. A 51 1918-1928 (1995).
10. Griem H. R., *Spectral Line Broadening by Plasmas* (Academic, New York, 1974).

11. Baranger M., in *Atomic and Molecular Processes*, edited by Bates D. R. (Academic, New York, 1962).
12. Griem H. R., Phys. Rev. **165**, 258–266 (1968).
13. Hey J. D. and Breger P., S. Afr. J. Phys. **5**, 111–121 (1982), J. Quant. Spectrosc. Radiat. Transfer **23**, 311–321 (1980), **24**, 349–364 (1980), **24**, 427–439 (1980), also in *Spectral Line Shapes*, edited by B. Wende (Walter de Gruyter, Berlin, 1981) pp. 191–200.
14. Dimitrijević M. S. and Sahal-Bréchot S., Astron. Astrophys. Suppl. Series, **93**, 359–371 (1992), **95**, 109–120 (1992), **107**, 349–351 (1994).
15. Konjević N. and Wiese W. L., J. Phys. Chem. Ref. Data **19**, 1307–1385 (1990).
16. Sanchez A., Blaha M., and Jones W. W., Phys. Rev. A **8**, 774–780 (1973).
17. Glenzer S., Uzelac N. I., and Kunze H.-J., Phys. Rev. E **45**, 8795–8802 (1992), also in *Spectral Line Shapes*, edited by Stamm R. and Talin B. (Nova Sci. Commack, New York, 1993), pp. 119–120
18. Glenzer S. and Kunze H.-J., Phys. Rev. A (1996) *in print.*
19. Lee R. W., in *Atomic Processes in Plasmas* eds. Marmor E. S. and Terry J. L. (AIP Conference Proceedings No. 257, New York, 1991) pp. 39–57.
20. Godbert L., Calisti A., Stamm R., Talin B., Glenzer S., Kunze H.-J., Nash J., Lee R. W., and Klein L., Phys. Rev. E **49**, 5889–5892 (1994).
21. Glenzer S., Wrubel Th., Büscher S., Kunze H.-J., Godbert L., Calisti A., Stamm R., Talin B., Nash J., Lee R. W., and Klein L., J. Phys. B **27**, 5507–5515 (1994).
22. Kunze H.-J., in *Spectral Line Shapes*, ed. Exton R. J. (Deepak, Hampton, Virginia, 1987) pp. 23–35.
23. Evans D. E., Plasma Phys. **12**, 573–584 (1970).
24. Wrubel Th., Glenzer S., Büscher S., and Kunze H.-J., J. Atmos. Terr. Phys. (1996) *in print.*
25. Spitzer L., Jr., *Physics of Fully Ionized Gases* (Interscience, New York, 1962).
26. DeSilva A. W., Baig T. J., Olivares I., and Kunze H.-J., Phys. Fluids B **4**, 458–464 (1992).
27. Glenzer S., in *Spectral Line Shapes*, eds. May D., Drummond R.,and Oks E. (AIP Conference Proceedings No. 328, New York, 1995) pp. 134–150.
28. Glenzer S., Hey J. D., and Kunze H.-J., J. Phys. B **27**, 413–422 (1994).
29. Büscher S., Glenzer S., Wrubel Th., and Kunze H.-J., J. Quant. Spectrosc. Radiat. Transfer **54**, 73–80 (1995).
30. Uzelac N. I., Glenzer S., Konjević N., Hey J. D., and Kunze H.-J., Phys. Rev. E **47**, 3623–3630 (1993).
31. Alexiou S. and Ralchenko Yu., Phys. Rev. A **49**, 3086–3088 (1994), **50**, 3553 (1994).
32. Alexiou S., Phys. Rev. Lett. **79**, 3406–3409 (1995).
33. Burke V. M., J. Phys. B **25**, 4917–4928 (1992).
34. Wrubel Th., Glenzer S., Büscher S., Kunze H.-J., and Alexiou S.,Astron. Astrophys. (1996) *in print.*